Cellular/Molecular

Rats Harboring S284L *Chrna4* Mutation Show Attenuation of Synaptic and Extrasynaptic GABAergic Transmission and Exhibit the Nocturnal Frontal Lobe Epilepsy Phenotype

Gang Zhu,[1,14]* Motohiro Okada,[1,6,14]* Shukuko Yoshida,[1,7] Shinya Ueno,[3,14] Fumiaki Mori,[4] Tomoko Takahara,[8] Ryo Saito,[8] Yoshiki Miura,[10] Akihiro Kishi,[11] Masahiko Tomiyama,[5] Akira Sato,[12] Toshio Kojima,[12,14] Goryu Fukuma,[9,14] Koichi Wakabayashi,[4,14] Koji Hase,[13] Hiroshi Ohno,[13,14] Hiroshi Kijima,[2] Yukio Takano,[8] Akihisa Mitsudome,[9] Sunao Kaneko,[1,14] and Shinichi Hirose[9,14]

Departments of [1]Neuropsychiatry, [2]Pathology and Bioscience, [3]Neurophysiology, [4]Neuropathology, and [5]Neurological Science, Institute of Brain Science, Graduate School of Medicine, Hirosaki University, Hirosaki 036-8562, Japan, [6]Division of Neuroscience, Graduate School of Medicine, Mie University, Tsu 514-8507, Japan, [7]Institute of Neuroscience and Molecular Biology, Shibata IRIKA, Hirosaki 036-8084, Japan, [8]Department of Pharmacology, Faculty of Pharmaceutical Sciences, and [9]Department of Pediatrics, School of Medicine, Fukuoka University, Fukuoka 814-0180, Japan, [10]Pharmacology Research Laboratories, Dainippon Sumitomo Pharmacy Company, Osaka 541-8524, Japan, [11]Discovery Research Laboratories III, Ono Pharmaceutical Company, Osaka 541-8564, Japan, [12]RIKEN Genomic Sciences Center and [13]RIKEN Research Center for Allergy and Immunology, Yokohama 230-0045, Japan, and [14]The Epilepsy Genetic Study Group,Hirosaki 036-8562 Japan

Mutations of genes encoding α4, β2, or α2 subunits (*CHRNA4*, *CHRNB2*, or *CHRNA2*, respectively) of nAChR [neuronal nicotinic ACh (acetylcholine) receptor] cause nocturnal frontal lobe epilepsy (NFLE) in human. NFLE-related seizures are seen exclusively during sleep and are characterized by three distinct seizure phenotypes: "paroxysmal arousals," "paroxysmal dystonia," and "episodic wandering." We generated transgenic rat strains that harbor a missense mutation S284L, which had been identified in *CHRNA4* in NFLE. The transgenic rats were free of biological abnormalities, such as dysmorphology in the CNS, and behavioral abnormalities. The mRNA level of the transgene (mutant *Chrna4*) was similar to the wild type, and no distorted expression was detected in the brain. However, the transgenic rats showed epileptic seizure phenotypes during slow-wave sleep (SWS) similar to those in NFLE exhibiting three characteristic seizure phenotypes and thus fulfilled the diagnostic criteria of human NFLE. The therapeutic response of these rats to conventional antiepileptic drugs also resembled that of NFLE patients with the S284L mutation. The rats exhibited two major abnormalities in neurotransmission: (1) attenuation of synaptic and extrasynaptic GABAergic transmission and (2) abnormal glutamate release during SWS. The currently available genetically engineered animal models of epilepsy are limited to mice; thus, our transgenic rats offer another dimension to the epilepsy research field.

Key words: **epilepsy; acetylcholine receptor; AChR; GABAergic modulation; glutamate; transgenic; transmission**

Introduction

In the past decade, genetic abnormalities of genes encoding ion channels expressed in the brain have been identified as the underlying causes of some 20 idiopathic epilepsy syndromes. Dysfunctions of ion channels reconstituted with mutations *in vitro* have been demonstrated in certain types of idiopathic epilepsy syndrome. Nonetheless, the mechanisms that link channel abnormalities and the epilepsy phenotypes are poorly understood. Animal models bearing mutations in genes encoding ion channels identified in human epilepsy and exhibiting the same epilepsy phenotype could be used to develop new treatments for epilepsy caused by channel abnormalities.

Nocturnal frontal lobe epilepsy (NFLE) (Steinlein et al., 1995, 1997, 2000; Hirose et al., 1999; De Fusco et al., 2000; Phillips et al., 2001; Bertrand et al., 2005) is one such idiopathic epilepsy syndrome with mutations of genes encoding ion channels. Mutations were identified in genes encoding α4, β2, and α2 subunits of nicotinic acetylcholine (ACh) receptors (nAChRs), *CHRNA4*, *CHRNB2*, and *CHRNA2*, respectively. The nAChR is a ligand-gated ion channel known to function as a pentamer consisting of three α and two βsubunits. The α4 and β2 subunits are major constituents of the nAChR in the brain.

Received June 20, 2008; revised Sept. 16, 2008; accepted Sept. 19, 2008.

Our work was conducted as part of a comprehensive project organized by The Epilepsy Genetic Study Group, Japan (Chairperson, S.K.) and was supported in part by the following: Grants-in-Aid for Scientific Research (S) 16109006, (A)18209035, (B) 18300137 and 18390316, (C) 17590856 and 20591361, for Exploratory Research 1659272 and 18659455, and "High-Tech Research Center" Project for Private Universities; matching fund subsidy from the Ministry of Education, Culture, Sports, Science, and Technology, 2006–2010; "The Research Center for the Molecular Pathomechanisms of Epilepsy, Fukuoka University" and a Research Grant (19A-6) for Nervous and Mental Disorders from the Ministry of Health, Labor, and Welfare and a grant from the Research Committee on Japan Epilepsy Research Foundation. We are indebted to our patients and their families for their helpful cooperation and encouragement in our research. We thank Akiyo Hamachi and Minako Yonetani (Fukuoka University) for their technical assistance.

*G.Z. and O.M. contributed equally to this work.

Correspondence should be addressed to Shinichi Hirose, Department of Pediatrics, Fukuoka University, 45-1, 7-chome, Nanakuma, Jonan-ku Fukuoka 814-0180, Japan. E-mail: hirose@fukuoka-u.ac.jp.

G. Zhu's present address: Department of Psychiatry, First Hospital of China Medical University, Shenyang 110001, China.

DOI:10.1523/JNEUROSCI.2961-08.2008

Two forms of NFLE have been described, autosomal dominant (ADNFLE) and sporadic (Phillips et al., 2000), although the clinical phenotype of NFLE is uniform, apart from minor differences. The seizures of NFLE are seen exclusively during sleep and characterized by three distinct seizure phenotypes, i.e., "paroxysmal arousals," "paroxysmal dystonia," and "episodic wandering."

In ADNFLE, three missense [S280F (Steinlein et al., 1995), S284L (Hirose et al., 1999), and T293I (Leniger et al., 2003)] and one insertional (insL) (Steinlein et al., 1997) mutation of *CHRNA4* (amino acid numbering of *CHRNA4* mutations used here is based on deduced amino acid sequence of human $\alpha 4$ subunit and accordingly differs from the original articles that were based on *Torpedo* sequence and nomenclature system), as well as three missense mutations [V287L (De Fusco et al., 2000), V287M (Phillips et al., 2001), and I312M (Bertrand et al., 2005)] of *CHRNB2* were found. Recently, a heterozygous missense I1287N of *CHRNA2* was described in a pedigree in which the phenotype of affected individuals was comparable with ADNFLE (Aridon et al., 2006). In particular, S284L was also identified in the sporadic form NFLE (Phillips et al., 2000). All ADNFLE/NFLE mutations were heterozygous and within the nAChR gating regulator or pore region (Wonnacott, 1997; Combi et al., 2004; Bertrand et al., 2005), and dysfunctions of the corresponding channel have been demonstrated *in vitro*.

To explore whether rats bearing mutations identified in human epilepsy exhibit seizure phenotypes similar to those in human, we generated transgenic (TG) rats that bear transgenes with a rat *Chrna4* missense S284L mutation, corresponding to a mutation identified in both ADNFLE and NFLE (Hirose et al., 1999; Ito et al., 2000; Phillips et al., 2000; Combi et al., 2004). The two strains demonstrated seizure phenotypes resembling those of human ADNFLE/NFLE, and, using one of the strains named "S284L-TG," we report here the underlying neurobiological abnormalities in these rats.

Materials and Methods

All animal experiments reported in this study were performed in accordance with the Guidelines for Animal Experimentation, Hirosaki University.

Generation of S284L transgenic rats

The rat cDNA of *Chrna4* was cloned from a rat fetal brain cDNA panel (Clontech) by PCR. The cDNA was subcloned with pCRII–TOPO vector (Invitrogen). Mutation S286L, corresponding to human S284L, was introduced in the rat cDNA in the same vector using the QuickChange site-direct mutagenesis kit (Stratagene). The nucleotide exchanges were c.856T>C and c.857C>T, which replace a Ser at 286 amino acid with a Leu according to the sequence of the rat *Chrna4* (GenBank accession number L31620). For generation of S284L-TG, the rat cDNA was excised from the vector with *Eco*RI and transferred into pCI–neo vector (Promega). The cDNA was excised from the pCI–neo vector with *Xho*I and *Not*I and transferred to a vector equipped with PDGF-β promoter constructed based on pCI–neo vector (a kind gift from Dr. Takashima, RIKEN, Wako, Japan). The PDGF-β promoter upstream of the multiple cloning site is a mammalian expression promoter that drives ectopic expression of transgenes mainly in the cortex and hippocampus, whereas the expression and distribution in transgenic animals are subject to change depending on the genetic location of transgenes (Kuteeva et al., 2004). The 4.0 kb fragment containing the PDGF-β promoter and S286L rat *Chrna4* cDNA and a 3′ untranslated sequence were prepared with *Sna*BI and *Nae*I and used as the transgene to generate S284L-TG on a Sprague Dawley background. Microinjection of the transgene and generation of S284L-TG was conducted at Japan SLC using standard procedures. Genomic DNA was prepared from tails of the animals by a standard method and direct sequencing with the primer pair TCTCCTGTCTCACCGTGCTG and CGTGTGTGTGCGTGGCGAGC.

Morphological studies

In these studies, 8-week-old and 2-year-old rats were killed by decapitation. The brains were harvested and then immersed in 4% paraformaldehyde with 0.1 M phosphate buffer, pH 7.4, for 24 h. The 4-μm-thick paraffin-embedded sections were stained with cresyl violet and also immunostained by the avidin–biotin–peroxidase complex (ABC) method using the Vectastain kit (Vector Laboratories), with anti-ssDNA (A4506; 1:100; DakoCytomation) as the primary antibody. The reaction was visualized with 0.02% 3,3′-diaminobenzidine tetrahydrochloride (DAB) and 0.005% H_2O_2 in 0.05 M Tris-HCl buffer, pH 7.6, for 10 min. Subsequently, the sections were counterstained with hematoxylin. For immunohistochemistry of $\alpha 4$ and $\beta 2$ subunits of nAChR, 8-week-old rats were anesthetized with sodium pentobarbital (20 mg/kg body weight, i.p.) and perfused transcardially with 0.1 M phosphate buffer, followed by a mixture of 2% paraformaldehyde and 0.3% glutaraldehyde in 0.1 M phosphate buffer. The brains were quickly removed, immersed in the same fixative for 3 h at 4°C, and stored overnight in 7.5% sucrose containing 0.1 M phosphate buffer. Vibratome sections (50 μm thick) were cut from the frontal cortex/striatum, hippocampus/thalamus, and occipital cortex/mesencephalon, immersed in 1% H_2O_2 for 15 min, blocked with 5% normal serum for 30 min, and then incubated with anti-nAChR $\alpha 4$ antibody prepared in guinea pig (AB5590; 1:500; Millipore Bioscience Research Reagents), rat (mAb299; 1:500; Sigma-Aldrich), or rabbit (BP2144; 1:100; Acris Antibodies) or with anti-nAChR $\beta 2$ antibody prepared in rat (mAb290; 1:500; Sigma-Aldrich) or rabbit (BP2147; 1:100; Acris Antibodies) for 24 h at 4°C, followed by incubation with a biotinylated secondary antibody (1:200; Vector Laboratories) for 1 h and ABC (1:200; Vector Laboratories) for 1 h. The reaction was developed with DAB (0.1 mg/ml) containing 0.0015% H_2O_2. For quantitative analysis, immunopositive cells were defined as those exhibiting somal staining. In each non-TG and S284L-TG, we counted the numbers of immunopositive cells in layers II/III or layer V of the frontal cortex and expressed the results as cell numbers per unit area (1 mm^2). The immunolabeled sections were postfixed in 1% osmium tetroxide in 0.1 M phosphate buffer for 1 h at 4°C, embedded in epoxy resin, cut, and then stained with uranyl acetate and lead citrate.

Both wild-type and S284L *Chrna4* mRNAs were investigated by using digoxigenin-labeled probes. The data presented here were obtained with antisense RNA probe synthesized to correspond to nucleotide residues 534–1008 of Sprague Dawley rat *Chrna4* cDNA (GenBank accession number L31620) (Le Novere et al., 1996). The procedures for probe labeling were similar to those reported previously (Hase et al., 2005; Zucker et al., 2005). The transgene expression (rat S284L *Chrna4* mRNA) was investigated by using ^{33}P-labeled oligonucleotide probes. The data presented here were obtained with an antisense oligonucleotide probe (5′-AAGAAGCAGCACCGAGATGCACAG) synthesized to correspond to nucleotide residues c.856T>C and c.857C>T of Sprague Dawley rat *Chrna4* cDNA (GenBank accession number L31620) (Le Novere et al., 1996). The procedures for probe labeling were similar to those reported previously (Mori et al., 2005).

Behavior

Locomotor activity. Locomotor activity was measured by NS-AS01 (Neuroscience Idea), which consists of an infrared ray sensor placed over the cage (34 $\times$ 33 $\times$ 17 cm), a signal amplification circuit, and a control unit. Rat movements were detected based on released infrared rays associated with body temperature. Each rat was removed from its home cage and placed individually in the observation cage. Locomotor activities of the rat kept in separate cages were measured simultaneously. Counts of locomotor activity were recorded in 5 min intervals over 60 h with a computer-linked analysis system (MDC; Neuroscience Idea) (Hirano et al., 2005). Rats were maintained under a 12 h light/dark cycle with lights on at 8:00 A.M. in a temperature- and humidity-controlled room. Food and water were provided *ad libitum*.

Rotarod performance for motor coordination. The rotarod performance was modified for non-TG and S284L-TG as described previously

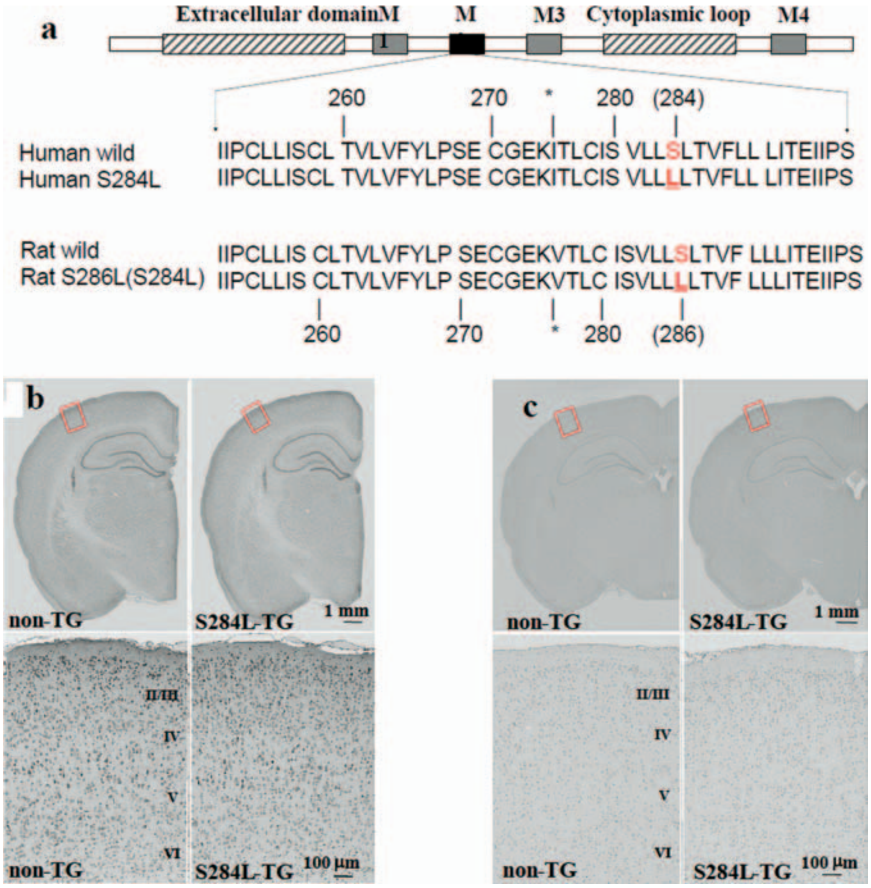

Figure 1. ***a***, Location of ADNFLE (S284L) mutations. The block diagram illustrates the α4 subunit of nAChR domains. Aligned amino acid sequences of the human and rat wild-type (wild) and S284L mutant M2 domains. The human and rat α4 subunit of nAChR M2 sequences differ by a single amino acid at position *. The mutated residues are shown in bold red. ***b***, Top, Cresyl violet-stained coronal cut sections of the left cerebral hemisphere of 2-year-old non-TG and S284L-TG. Bottom, Higher-magnification views of the cortical areas marked by the rectangles. ***c***, Top, ssDNA immunostained coronal sections of the left cerebral hemisphere of 2-year-old non-TG and S284L-TG. Bottom, Higher-magnification views of the cortical areas marked by the rectangles.

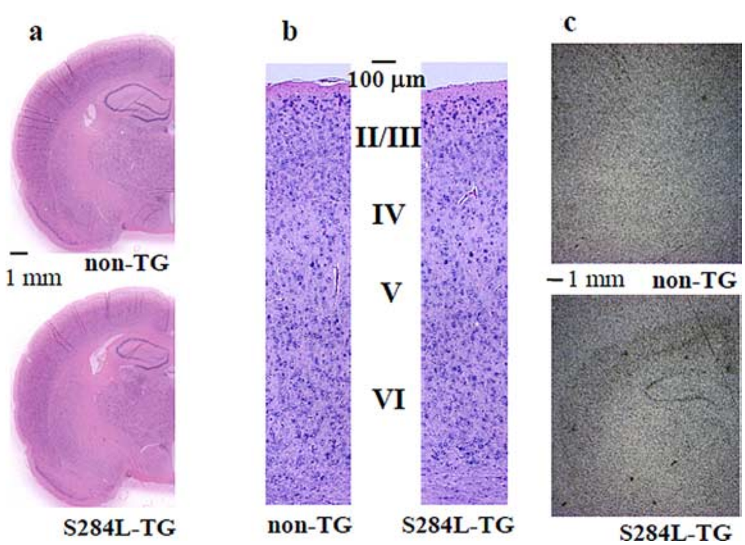

Figure 2. ***a***, *In situ* hybridization analysis using digoxigenin-labeled probes shows the expression of both wild-type with S284L mutant *Chrna4* mRNA in brain. ***b***, Light micrographs of digoxigenin-labeled probe-positive cells (both wild-type with S284L mutant *Chrna4* mRNA-sensitive probe) in the sensorimotor cortex. ***c***, The mRNA expression of transgene (S284L *Chrna4* mRNA) in brain using S284L *Chrna4* mRNA-selective ^{33}P-labeled oligonucleotide probes.

(Mishima et al., 2004). Both littermates were placed on the rotating rod (7 cm diameter; Neuroscience Inc.) with a nonskid surface, and the latency to fall was measured for up to 2 min. The rotating speed was 5 rpm.

Hot-plate test for nociceptive sensory function. This test was performed using a hot-plate apparatus (DS-37; Ugo Basile), maintained at 55 ± 0.1°C. Responses were measured as the latency to first hindpaw licking. The latency was determined individually as the mean of three trials (Harasawa et al., 2003).

Traction meter for muscle tone. The traction meter (Neuroscience Inc.) consists of a detector (48.5 × 26 × 10 cm) of muscle tone with stainless grids (2 mm in diameter, 29 × 16 cm) connected to a spring and a printer. The stainless grids can freely rotate by themselves. Each rat was placed on the 2 × 2 cm stainless grids of the apparatus, and the experimenter slowly pulled the tail in parallel at a constant speed. The forepaw resistance was measured by the detector as muscle tone (Mishima et al., 2004).

Electrocorticography

For polygraphic electrocorticography (for recording interictal discharge), we implanted twisted bipolar stainless steel wire electrodes, insulated except at their tips, into the sensorimotor cortex [anterior (A), 2.0 mm; lateral (L), 4.0 mm; ventral (V), −1.8 mm relative to bregma], right basolateral amygdala (A, −2.8 mm; L, 5.0 mm; V, −7.5 mm), and left ventrolateral nucleus of the thalamus (A, −2.3; L, 1.8 mm; V, −5.4 mm). For free moving electrocorticography (to record epileptic wandering), we screwed the recording and reference electrodes on the skull over the frontal and occipital regions. After baseline recording, we administered carbamazepine (25 mg/kg/d) or zonisamide (30 mg/kg/d) orally once daily and then continuously recorded the electrocorticogram throughout the day, using a telemetry system (Unimec) (Okada et al., 2003).

Pharmacological analysis of seizure susceptibility

The experiment was performed as described previously (Tecott et al., 1995; Nakatsu et al., 2004). In brief, pentylenetetrazole (4 mg/kg) or bicuculline (0.05 mg/kg) was infused at a constant rate into the tail vein of non-TG or S284L-TG rats. The doses of pentylenetetrazole and bicuculline (milligrams per kilogram) were determined by examining the stage of seizure, which appears on the vertical line. The stages for pentylenetetrazole-induced seizure were as follows: first twitches of head and body, mild clonic behavior, and tonic flexion behavior. The stages for bicuculline-induced seizure were as follows: first twitch, mild clonic behavior, jumping, and tonic flexion behavior.

Determination of neurotransmitter release

A concentric I-type dialysis probe fixed with stainless steel wire electrodes (0.22 mm diameter; 3 mm exposed membrane; Eicom) was implanted in the frontal cortex under halothane anesthesia (1.5% mixture of halothane and O_2 with N_2O), and the perfusion experiments commenced 36 h after recovery from anesthesia. The perfusion rate was set at 1 μl/min, using modified Ringer's solution composed of the following (in mM): 145 Na^+, 2.7 K^+, 1.2 Ca^{2+}, 1.0 Mg^{2+}, and 154.4 Cl^-, buffered with 2 mM phosphate buffer and 1.1 mM Tris buffer, pH 7.40. Glutamate and GABA concentrations in the perfusate were determined as described previously (Okada et al., 2001, 2003; Nakatsu et al., 2004), using microdialysis and HPLC with fluorescence detection (Jasco) (Nakatsu et al., 2004).

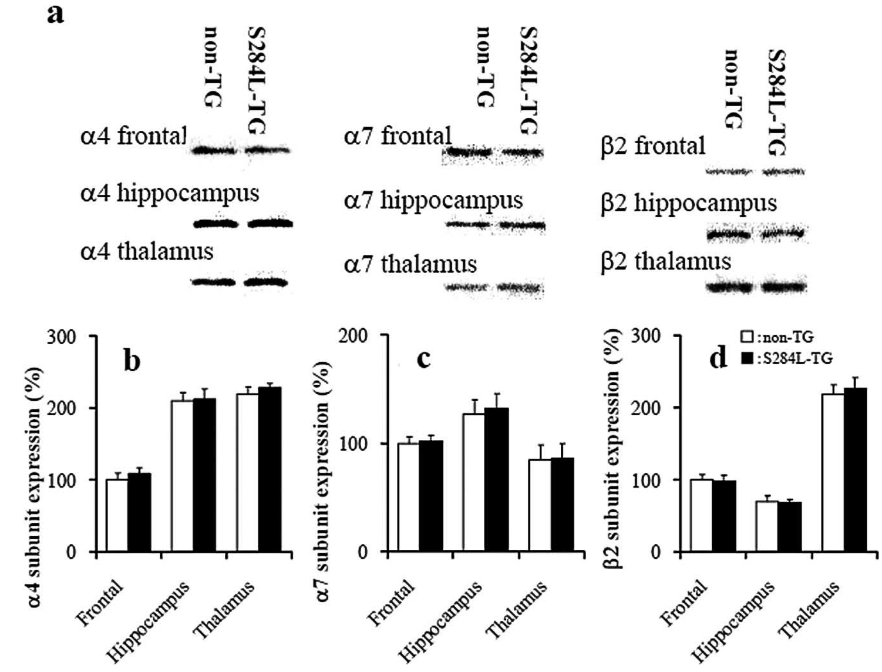

Figure 3. ***a***, Western blotting of α4, α7, and β2 subunits of nAChR in frontal, hippocampal, and thalamic total lysates. ***b–d***, Quantitative analysis of the amounts of α4 (***b***), α7 (***c***), and β2 subunit (***d***) proteins in frontal, hippocampal, and thalamic total lysates. Data are mean ± SD ($n = 9$) of percentage control (the signal of frontal total lysate in non-TG).

Brain slice preparation and neurotransmission analysis

Coronal cortical slices (400 μm thick) were obtained from 3- to 4-week-old rats (Yamamoto et al., 2007), transferred to a recording chamber, superfused (2.5 ml/min) with gassed (95% O_2–5% CO_2) artificial CSF (ACSF) (in mM: 126 NaCl, 2.5 KCl, 2 $CaCl_2$, 2 $MgSO_4$, 1.25 NaH_2PO_4, 26 $NaHCO_3$, and 20 glucose at pH 7.4), and maintained at 30°C. During monitoring of spontaneous IPSC (sIPSC) and GABAergic tonic inhibition, ACSF containing the inhibitors of muscarinic receptor atropine (1 μM), α7-nAChRs, and methyllycaconitine (MLA) (0.1 μM), the NMDA receptor D(−)-2-amino-5-phosphonopentanoic acid (D-APV) (50 μM), the AMPA receptor 6-cyano-7-nitroquinoxaline-2,3-dione (CNQX) (10 μM), and the $GABA_B$ receptor CGP55845 [(2*S*)-3-[(15)-1-(3,4-dichlorophenyl)ethyl]amino-2-hydroxypropyl)(phenylmethyl)phosphinic acid] (3 μM) were used for perfusion. Patch electrodes were prepared from thin-walled borosilicate glass tubing using a pipette puller, with tip resistances of 4–5 MΩ when filled with a high Cl^- solution containing the following (in mM): 130 CsCl, 3 $MgCl_2$, 0.5 EGTA, 10 HEPES, 3 $Mg(ATP)_2$, 0.4 GTP, and 5 *N*-ethyl lidocaine (QX-314). The pH was adjusted to 7.3 with CsOH. Whole-cell patch-clamp recordings were made from visually identified layer V pyramidal neurons of the sensorimotor cortex. Under these experimental conditions, GABAergic sIPSC were reversed at ∼0 mV [the E_{Cl} predicted by the Goldman–Hodgkin–Katz (GHK) equation]. With cells voltage clamped at −60 mV in the presence of sEPSC blockers (CNQX and D-APV), the GABAergic IPSC appeared as an inward current. During monitoring of sEPSC, ACSF containing atropine (1 μM), MLA (0.1 μM), and CGP55845 (3 μM) was superfused. Patch pipettes were filled with low Cl^- solution containing the following (in mM): 150 potassium methanesulfonate, 5 KCl, 3 $MgCl_2$ 0.5 EGTA, 10 HEPES, 3 $Mg(ATP)_2$, 0.4 GTP, and 5 QX-314. Under these conditions, GABAergic sIPSCs were reversed at approximately −65 mV (the E_{cation} predicted by the GHK equation). Thus, with cells voltage clamped at −65 mV, sEPSCs were only recorded as an inward current. The recorded currents were filtered at 2 kHz and digitized at 5–10 kHz using DigiData1322A and pClamp 9.2 software (Molecular Devices). Synaptic currents and tonic GABA currents were measured and analyzed as described previously (Glykys and Mody, 2007; Yamamoto et al., 2007). sIPSCs and sEPSCs were examined by constructing cumulative probability distributions for 1 min epochs, immediately before (control) and from 4–5 min of drug application and were compared using the Kolmogorov–Smirnoff (K–S) test with a single neuron. Summarized data obtained from several neurons are expressed as mean ± SD, after normalization with the control. Each control or drug-applied value is the mean of all synaptic events during 1 min epochs. Differences in amplitude and frequency distribution were tested using a Student's paired *t* test or the Steel–Dwass test for multiple comparisons. Values of $p < 0.05$ were considered significant.

The glutamatergic AMPA and NMDA field EPSPs (fEPSPs) were monitored using the MED64 system (Alpha-MED Sciences), equipped with MED-P5155 probes (150 μm interpolar distance for the electrodes in an 8 × 8 array) (Okada et al., 2003; Nakatsu et al., 2004). The superfusion medium was Mg^{2+}-free ACSF composed of the following (in mM): 126 NaCl, 2.5 KCl, 2 $CaCl_2$, 1.25 NaH_2PO_4, 26 $NaHCO_3$, and 20 glucose (pH 7.4 when bubbled with 95% O_2–5% CO_2). The layer II/III sensorimotor cortex was stimulated by one single planar microelectrode with bipolar constant current pulses (60 μA, 0.1 ms), and fEPSPs were selectively recorded from layer V.

Western blotting

SDS-PAGE was performed according to standard procedures using Bio-Rad Protean III. The bound antibody, anti-nAChR α4 subunit (mAb299; Sigma-Aldrich), anti-nAChR β2 subunit (mAb290; Sigma-Aldrich), and anti-nAChR α7 subunit (mAb319; Sigma-Aldrich), were labeled by biotin-conjugated affinity-purified secondary antibody (Millipore Bioscience Research Reagents) and then labeled by secondary antibody bound to streptavidin–cyanine 3 (Cedarlane) for visualization using molecular imager FX pro (Bio-Rad).

Laser capture microdissection and single-cell reverse-transcription quantitative PCR

Coronal 8-μm-thick sections from non-TG and S284L-TG brains were cut on a cryostat and thaw mounted on noncoated glass slides. Sections were stained using the HistoGene LCM Frozen Section Staining kit (Arcturus). After visualization, individual pyramidal neurons, oligodendrocytes, and astrocytes in layer V of sensorimotor cortex were dissected out using the PixCell II LCM instrument (Arcturus), diameter 7.5 μm, onto CapSure Micro LCM caps (Arcturus). The dissected cells were solubilized from the cap in extraction buffer provided with the Pico Pure RNA isolation kit (Arcturus) for 30 min at 42°C and stored at −80°C. Each sample underwent RNA extraction according to the instructions provided by the manufacturer, including DNase treatment using RNase-Free DNase set (Qiagen) (Zucker et al., 2005). Each RNA was reverse transcribed with random hexamer using Moloney murine leukemia virus reverse transcriptase (Applied Biosystems). Real-time PCR was performed in the TaqMan 7000 Sequence Detection System (Applied Biosystems). We designed PCR primers and TaqMan MGB probes against *Chrna4* (GenBank accession number L31620), myelin basic protein (*Mbp*) (GenBank accession number NM_001025289), and glial fibrillary acidic protein (*Gfap*) (GenBank accession number NM_017009) using the PrimerExpress 2.0 software (Applied Biosystems).

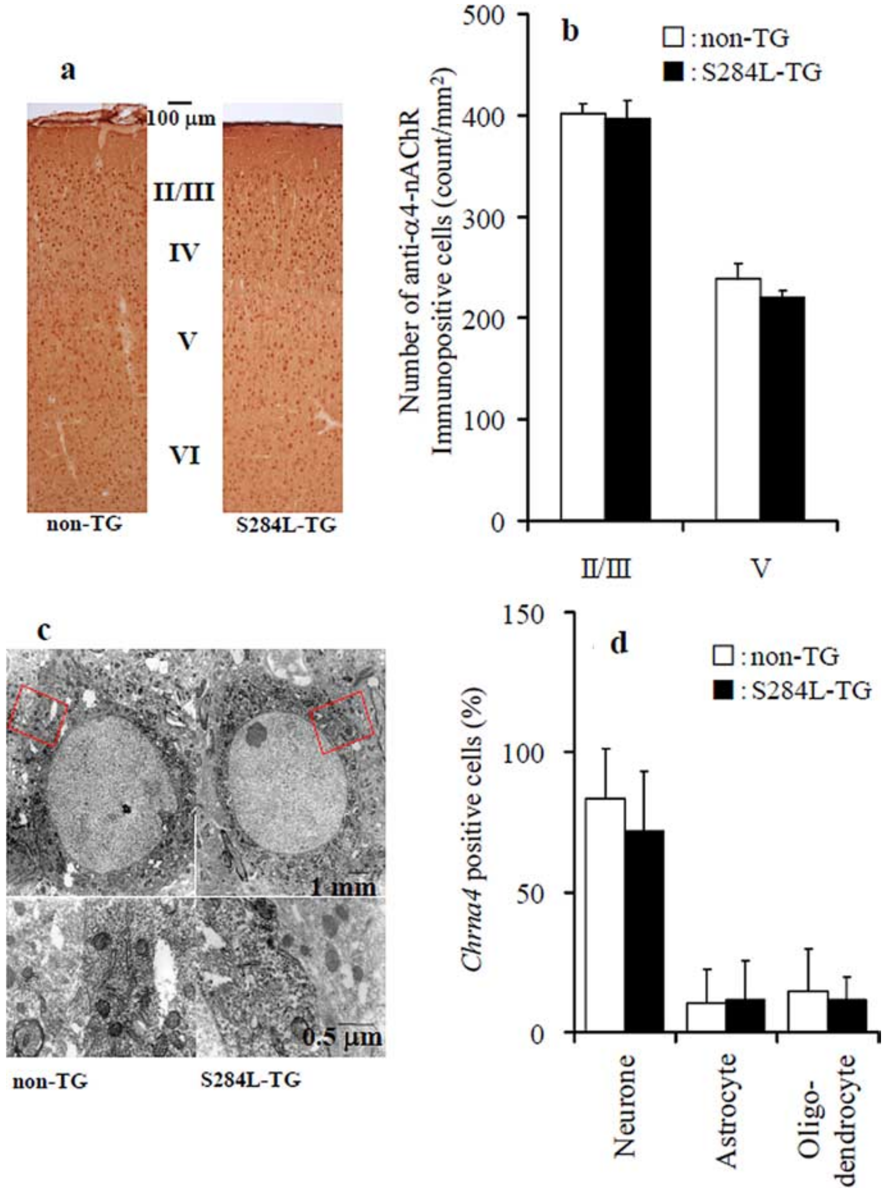

Figure 4. ***a***, Light micrographs of α4-nAChR immunoreactivity in sensorimotor cortex. Note the immunostained neuronal cell bodies and apical dendrites in layers II–VI. ***b***, Numbers of anti-nAChR α4-immunopositive cells in layers II/III and layer V in the frontal cortices of non-TG and S284L-TG ($n = 12$). ***c***, Top, Immunoelectron microscopy of the sensorimotor cortices labeled with anti-nAChR α4 antibody (mAb299). Immunoreactivity of α4 subunit of nAChR is present in the perikarya. Bottom, Higher-magnification views of areas marked by the rectangles. ***d***, *Chrna4* mRNA-positive populations of pyramidal neurons, *Gfap* mRNA-positive astrocytes, and *Mbp* mRNA-positive oligodendrocytes in the sensorimotor cortical layer V were determined using laser capture microdissection with single-cell reverse-transcription PCR. Data are mean $\pm$ SD of six rats (Wilcoxon rank sum test).

Results

Generation and characterization of S284L-TG

We constructed the rat cDNA of *Chrna4* (GenBank accession number L31620) bearing c.856T>C:c.857C>T mutations to generate an amino acid exchange homologous to human S284L (Fig. 1*a*). We then introduced the mutant cDNA preceded by the PDGF-β promoter sequence (Kuteeva et al., 2004) into rat oocytes by the microinjection method (Matsushima et al., 2002). We obtained two transgenic strains. The proportion of transgenic rats among littermates followed the Mendelian law. The non-TG and transgenic rat littermates were equally fertile and survived at least 2 years. The two strains resembled the human ADNFLE/NFLE phenotypically, and thus one of the strains, named S284L-TG, was used for further characterization of the TG.

Histological examination revealed no abnormality in the overall structure of the brain of S284L-TG (from 8 to 100 weeks of age) (Fig. 1*b*). In addition, no clear increase in apoptotic ssDNA-positive cells was noted in S284L-TG compared with non-TG (from 8 to 100 weeks of age) (Fig. 1*c*). There were no differences between non-TG and S284L-TG in general behaviors and sensorimotor functions when assessed by rotarod test for motor coordination, open-field test for analysis of locomotor activity and circadian rhythm, hot-plate test for analysis of sensory function, and traction meter test for muscle tone (data not shown) (Mishima et al., 2004).

No serious distortion of transgene and mutant nAChR expression in S284L-TG

In situ hybridization using nonselective probe (sensitive to both wild-type and S284L mutant *Chrna4* mRNA) revealed no differences in the expression of *Chrna4* mRNA in the brain between non-TG and S284L-TG (Fig. 2*a*,*b*). The total amount of *Chrna4* mRNA (wild-type plus S284L *Chrna4*) in the frontal cortex of S284L-TG was almost equal to that in non-TG. The expression of wild-type versus S284L *Chrna4* was 45 versus 55%. Furthermore, *in situ* hybridization using S284L *Chrna4*-selective probe indicated that the transgene was expressed predominantly in the cortex and hippocampus (Fig. 2*c*). The amounts of α4-, α7-, and β2-nAChR subunits in frontal, hippocampal, and thalamic total lysates in S284L-TG were comparable with those in non-TG at the protein level (Fig. 3*a*–*d*).

In the sensorimotor cortex, *in situ* hybridization and immunohistochemical analyses showed no differences in the expression of *Chrna4* or α4-nAChR subunit protein between non-TG and S284L-TG (Figs. 2*b*, 4*a*). There was no significant difference in the numbers of nAChR α4-immunopositive neurons between non-TG and S284L-TG (Fig. 4*b*). Electron microscopic examination showed the presence of immunoreactive α4-nAChR subunit in neuronal perikarya mainly associated with rough endoplasmic reticulum, cytoplasmic matrix, and plasma membrane (Schröder et al., 1989; Nakayama et al., 1995) (Fig. 4*c*).

We also examined any ectopic expression of the transgene in neurons and glial cells using laser-capture microdissection with single-cell reverse-transcription quantitative PCR. The mRNAs of both wild-type and S284L *Chrna4* were identified in pyramidal neurons, astrocytes (glial fibrillary acidic protein mRNA-positive) (Zucker et al., 2005) and oligodendrocytes (myelin basic protein mRNA-positive) (Zucker et al., 2005) in the sensorimotor cortex. No distorted expression of wild-type or S284L *Chrna4* was observed in the three cell populations examined (Fig. 4*d*).

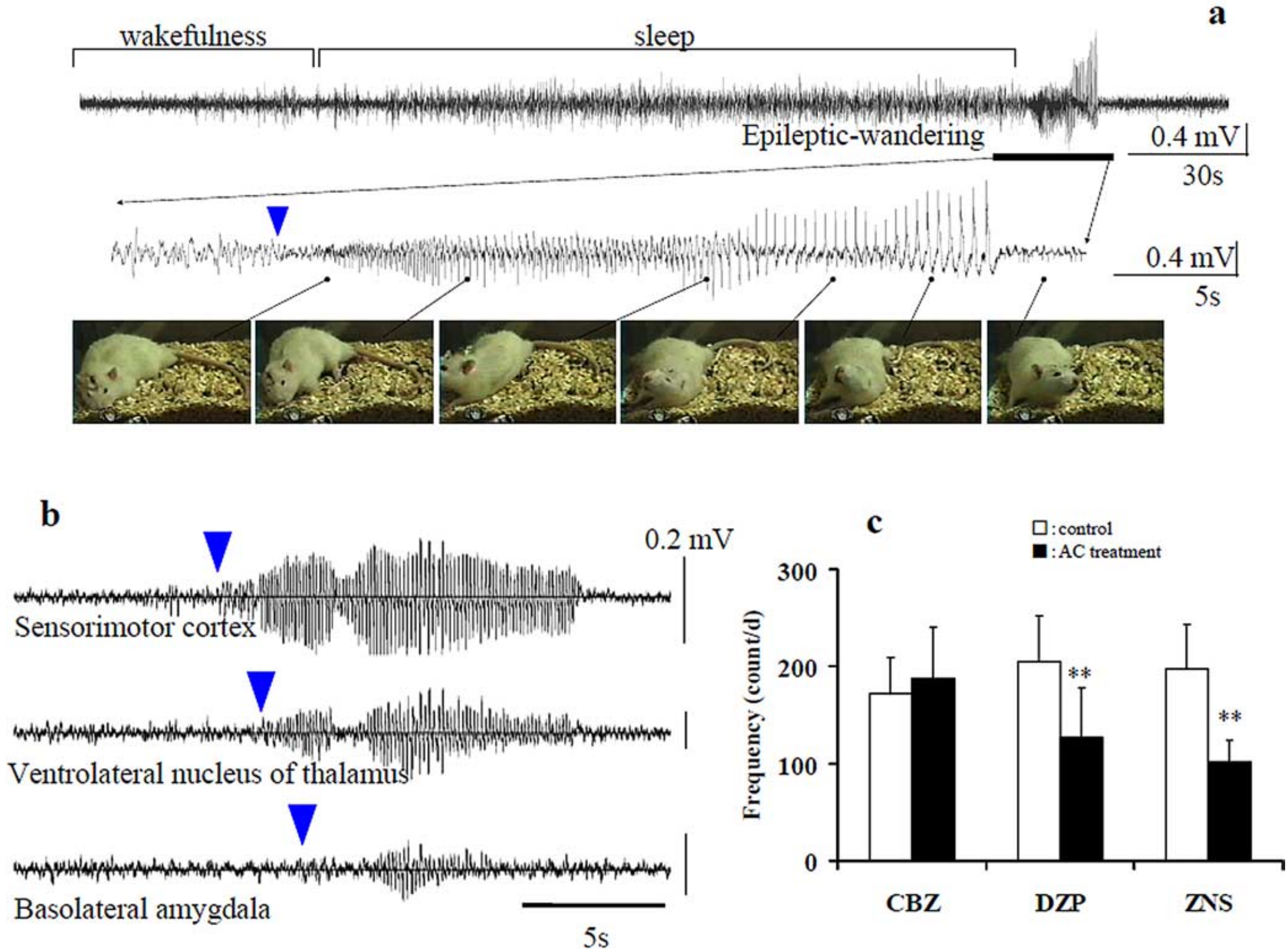

Figure 5. ***a***, Typical electrocorticograms of the sensorimotor cortex of S284L-TG during epileptic wandering were monitored using the single-channel telemetric system. The photographs indicate the behavioral abnormalities during epileptic wandering. The blue arrowhead indicates the onset of ictal discharge in sensorimotor cortex. The spontaneous epileptic seizures during SWS are of three distinct types: paroxysmal arousals, brief episodes characterized by sudden frightened expression; paroxysmal dystonia, manifested as brief episodes of dystonic posturing; and epileptic wandering, episodes of longer duration (0.5–3 min) with head shaking accompanied by stereotyped paroxysmal ambulation and bizarre movements, similar to the respective ADNFLE/NFLE seizures, nocturnal paroxysmal arousals, nocturnal paroxysmal dystonia, and episodic nocturnal wandering. The onset of ictal discharges was synchronized with seizure behaviors. Similar to ADNFLE/NFLE patients, all three types of seizures frequently occurred in the same individual rat. Spontaneous ADNFLE/NFLE seizures appeared at 8 weeks of age. The frequency of ADNFLE/NFLE seizures was once a week. ***b***, Typical electrocorticograms during interictal discharge monitored using multichannel electrocorticography in the sensorimotor cortex, ventrolateral nucleus of thalamus, and basolateral amygdala. The blue arrowheads indicate the onset of interictal discharge in each brain region. The frequent interictal discharges originating from the sensorimotor cortex were recorded during SWS and propagated to the ventrolateral nucleus of the thalamus and basolateral amygdala. Interictal discharges appeared at 6 weeks of age, and their frequency increased with age; at 8 weeks of age, their frequency was >150/d. ***c***, Effects of 2 week administration of anticonvulsants (from 8 to 10 weeks of age), carbamazepine (CBZ; 25 mg/kg/d), diazepam (DZP; 1 mg/kg/d), and zonisamide (ZNS; 30 mg/kg/d), on the frequency (count per day) of interictal discharge in S284L-TG at before (control) and during anticonvulsants treatment (AC treatment). Data are mean $\pm$ SD ($n = 10$). $^{**}p < 0.01$ (Wilcoxon rank sum test). The frequency of epileptic discharge was 198.0 $\pm$ 56.3/d in S284L-TG before treatment.

The expression of S284L *Chrna4* mRNA was observed in all *Chrna4* mRNA-positive pyramidal neurons (wild type, 40%; S284L, 60%), astrocytes (wild type, 56%; S284L, 44%), and oligodendrocytes (wild type, 59%; S284L, 41%) in the sensorimotor cortex of S284L-TG. These results indicate no serious distorted expression of S284L mutant α4-nAChR subunit protein.

Epileptic phenotypes of S284L-TG

S284L-TG developed three distinct spontaneous epileptic seizures types during slow-wave sleep (SWS) phase: paroxysmal arousals, brief episodes characterized by sudden frightened expression (supplemental figure, available at www.jneurosci.org); paroxysmal dystonia, manifested as brief episodes of dystonic posturing (supplemental figure, available at www.jneurosci.org); and epileptic wandering, episodes of longer duration (0.5–3 min) with head shaking accompanied by stereotyped paroxysmal ambulation and bizarre movements (Fig. 5*a*), similar to the respective ADNFLE/NFLE seizures of "nocturnal paroxysmal arousals," "nocturnal paroxysmal dystonia," and "episodic nocturnal wandering" (Provini et al., 1999; Combi et al., 2004). The onset of ictal discharges was synchronized with seizure behaviors. The frequencies of these three typical ADNFLE/NFLE seizures were once a week. Similar to ADNFLE/NFLE patients (Provini et al., 1999; Combi et al., 2004), all three types of seizures occurred frequently in the same individual rat. Electrocorticography showed that the focus of interictal discharge was in the sensorimotor cortex (Fig. 5*b*). The onset of interictal discharges was 6 weeks of age; however, the onset of spontaneous epileptic seizure was preceded by that of interictal discharge in the same individual S284L-TG. At 8 weeks of age, >90% of S284L-TG exhibited spontaneous epileptic seizures during SWS, and the frequency of interictal discharges was ~200 times a day (Fig. 5*c*). The majority

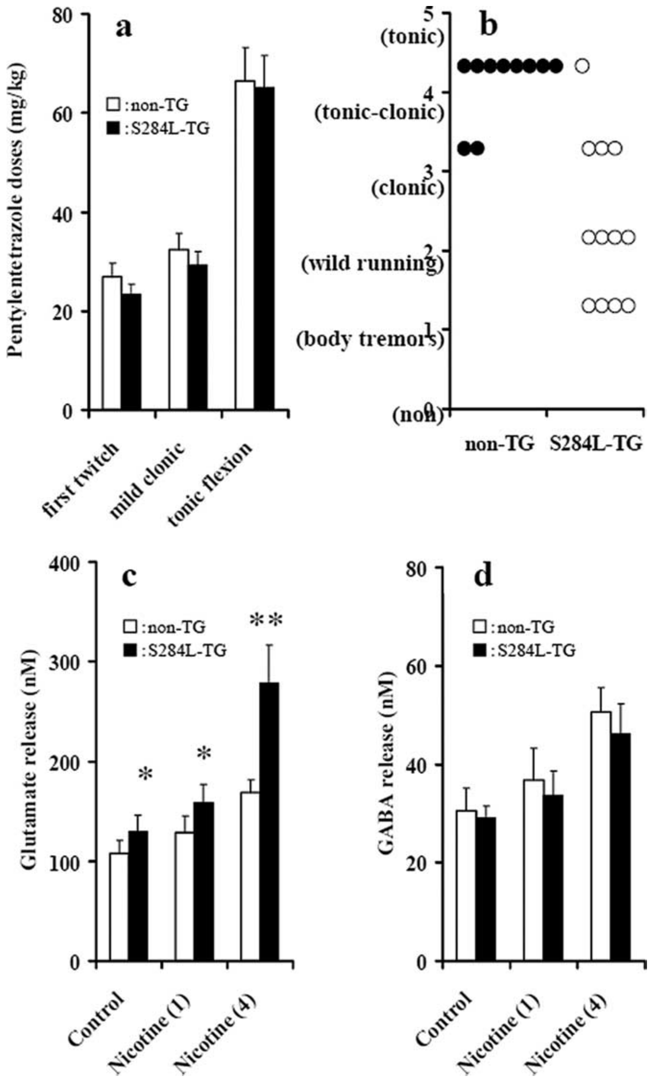

Figure 6. ***a***, Dose-dependent seizure test induced by intravenous administration of pentylenetetrazole in S284L-TG and non-TG. The ordinate shows the required doses of pentylenetetrazole (milligrams per kilogram), when a specific type of behavior was noted ($n = 12$ rats). There were no significant differences between the two groups (Student's *t* test). ***b***, The seizure score induced by 4 mg/kg (i.p.) nicotine. The scored nicotine-induced behaviors include the following: (1) head and body tremors and/or near loss of righting response; (2) any combination of severe tremors, wild running, and complete loss of righting response; (3) clonic seizures; (4) tonic-clonic seizures; (5) tonic seizures. Frontal release of glutamate (***c***) and GABA (***d***) during 1 mg/kg (1) and 4 mg/kg (4) nicotine-induced seizure. Data are mean ± SD of 12 rats. $^{**}p < 0.01$ (Student's *t* test).

of both ictal and interictal discharges appeared during SWS but did not necessarily occur after sleep spindles (Fig. 5*a*,*b*). The frequent interictal discharges originating from the sensorimotor cortex were recorded during SWS, which propagated to the ventrolateral nucleus of the thalamus and basolateral amygdala (Fig. 5*b*).

Similar to ADNFLE/NFLE patients with S284L (Provini et al., 1999; Ito et al., 2000; Phillips et al., 2000; Combi et al., 2004), 2 week treatment with diazepam and zonisamide at therapeutically relevant doses reduced the frequency of interictal discharge by 43 and 48% in S284L-TG, respectively, whereas carbamazepine was not effective (Fig. 5*c*).

S284L-TG showed no hypersensitivity to conventional generalized seizure tests induced by pentylenetetrazole (Fig. 6*a*), photo stimulation, audio stimulation, or maximal electroshock (data not shown) compared with non-TG. Surprisingly, no difference was observed between S284L-TG and non-TG in the latency of nicotine-induced (4 mg/kg, i.p.) seizures (data not shown); instead, the nicotine-induced seizures seen in S284L-TG were mainly partial seizures, whereas those in non-TG were generalized seizures (Fig. 6*b*). Administration of nicotine (1 and 4 mg/kg, i.p.) dose dependently increased extracellular levels of glutamate and GABA in the frontal cortex of non-TG and S284L-TG (Fig. 6*c*,*d*). The nicotine-induced rise in extracellular glutamate level of S284L-TG was larger than that of non-TG (Fig. 6*c*); however, there was no difference between nicotine-induced elevation of extracellular GABA levels of non-TG and S284L-TG (Fig. 6*d*).

Attenuated GABAergic transmission in sensorimotor cortex of S284L-TG

To characterize the nAChR function in the epileptic focus region, we monitored both GABAergic sIPSC and glutamatergic sEPSC of pyramidal neurons in the sensorimotor cortex using slice patch-clamp technique. In the sensorimotor cortical layer V, a predominant initiator and propagator of synchronous epileptic activities (Connors, 1997), there was no difference in resting membrane potential between S284L-TG (-65.8 ± 4.1 mV) and non-TG (-66.6 ± 3.8 mV).

The absolute values of frequency and amplitude of spontaneous sIPSCs were compared between S284L-TG and non-TG under the blockade of AMPA/glutamate receptor, NMDA/glutamate receptor, $GABA_B$ receptor, muscarinic ACh receptor, and α7-nAChR. The frequency of sIPSCs was significantly lower in S284L-TG (4.53 ± 2.85 Hz; $n = 6$) than in non-TG (16.96 ± 5.4 Hz; $n = 5$). Conversely, the amplitude of sIPSCs tended to be lower in S284L-TG (-21.22 ± 11.22 pA; $n = 6$) than in non-TG (-35.32 ± 16.86 pA; $n = 5$), although this was not statistically significant.

Under the same blockade, cumulative probability distributions for peak sIPSC amplitude and mean interevent interval in control condition and during application of nicotine were examined for non-TG and S284L-TG. At 10 μM nicotine application, mean peak amplitude was significantly increased ($p < 0.01$, K–S test), and mean interevent interval for sIPSCs was significantly decreased in non-TG ($p < 0.01$, K–S test) but not in S284L-TG. Nicotine concentration of 10 μM is very high for the $\alpha4\beta2$-nAChR and could cause both saturation of the evoked current and receptor desensitization. Because this high nicotine concentration was bath applied, one cannot rule out that nicotine-induced depression of the $\alpha4\beta2$-nAChR activity as well as nicotine-induced activation of the α7-nAChRs. Accordingly, we also tested the effects of lower concentrations of nicotine. At 1 μM, nicotine did not change the frequency or the amplitude of sIPSCs, and these effects were similar in non-TG and S284L-TG (Fig. 7*c*–*f*). In addition, these effects of nicotine on sIPSC were not observed in sensorimotor cortical layers II/III pyramidal neurons of S284L-TG (Fig. 8*c*).

In contrast to sIPSC, under the blockade of $GABA_B$ receptor, muscarinic ACh receptor and α7-nAChR, application of nicotine affected neither the frequency nor amplitude of sEPSC of non-TG and S284L-TG (Fig. 7*g*,*h*). However, nicotine-activated extrasynaptic GABAergic inhibition (tonic inhibition) seen in non-TG (Rossi et al., 2003; Farrant and Nusser, 2005) was absent in S284L-TG (Fig. 8*a*). Thus, delta of holding currents by application of nicotine in non-TG and in S284L-TG were -24.5 ± 11.6 and -5.5 ± 3.4 pA, respectively (mean ± SD of six neurons; $p < 0.05$, Student's *t* test).

S284L-TG showed loss of function of activation of GABAergic transmission in both synaptic and extrasynaptic inhibitions without changing glutamatergic transmission before 4 weeks of age (i.e., before onset of spontaneous seizure).

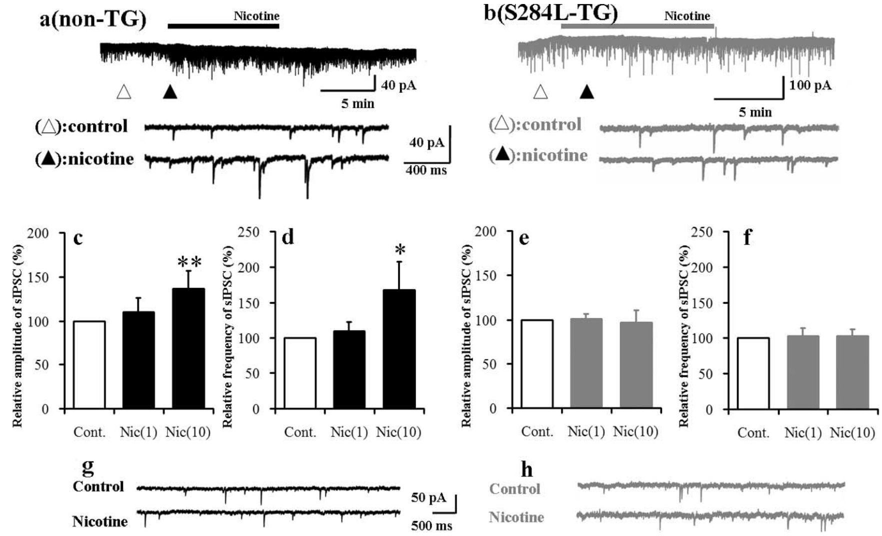

Figure 7. Typical traces of sIPSC in response to 10 μM nicotine in sensorimotor cortical layer V pyramidal neurons of non-TG (***a***, black) and S284L-TG (***b***, gray). After recording the control state (△), the ACSF perfusion medium was replaced with nicotine-containing ACSF (▲). Bar graphs summarize dose-related effects of nicotine (1 and 10 μM) on sIPSC amplitude (***c***, ***e***) and frequency (***d***, ***f***) (each shown as mean percentage control). Data are mean ± SD of six neurons. $^{*}p < 0.05$, $^{**}p < 0.01$ (Steel–Dwass test for multiple comparisons). As for sEPSC, typical traces of sEPSC to 10 μM nicotine in sensorimotor cortical layer V pyramidal neurons in non-TG (***g***, black) and S284L-TG (***h***, gray). Nicotine did not alter the mean amplitude and frequency of sEPSC in non-TG (***d***) and S284L-TG (***f***) (Steel–Dwass test for multiple comparisons).

Enhanced propagation of neuronal excitability in sensorimotor cortex of S284L-TG

To study the propagation of neuronal hyperexcitability from the focus region, we examined the effect of nicotine on fEPSP using multielectrode monitoring system (Aramakis and Metherate, 1998; Okada et al., 2003). First, we compared the propagation of bipolar stimulation-induced fEPSP in cerebral cortex layer II in S284L-TG and non-TG rats. The number of electrodes in which fEPSPs were elicited was counted. Bipolar stimulation evoked fEPSP at 49.8 ± 7.4 (n = 6) electrodes of the MED64 system in S284L-TG and at 45.0 ± 6.3 (n = 4) in non-TG. However, there was no significant difference in fEPSP propagation between S284L-TG and non-TG rats. Nicotine concentration dependently enhanced fEPSP in the sensorimotor cortex of both non-TG and S284L-TG. In particular, nicotine significantly enhanced fEPSP associated with AMPA/glutamate receptor (fEPSP/AMPA) in the sensorimotor cortex of S284L-TG compared with non-TG, whereas there was no difference between the two groups in nicotine-induced fEPSP associated with NMDA/glutamate receptors (fEPSP/NMDA) (see Fig. 10*a–c*). The fEPSP/NMDA was enhanced by α7-nAChRs but unaffected by $\alpha 4\beta 2$-nAChRs in the sensorimotor cortex of both S284L-TG and non-TG (Aramakis and Metherate, 1998; Bayazitov and Kleschevnikov, 2000) (Fig. 9*a–d*). Pretreatment with $GABA_A$ receptor inhibitor abolished the augmentation of nicotine-induced fEPSP/AMPA in S284L-TG (Fig. 9*a–d*). Therefore, S284L-TG showed enhanced excitatory glutamatergic transmission induced by attenuation of GABAergic synaptic and extrasynaptic inhibitions before 4 weeks of age (i.e., before the onset of spontaneous seizure).

Dysfunction of neurotransmitter release associated with circadian rhythm

To address the question why ADNFLE/NFLE seizures occur predominantly during SWS, we studied the frontal neurotransmitter release associated with circadian rhythm in both predevelopment of spontaneous seizure (4 weeks of age) and postdevelopment of spontaneous seizure (8 weeks of age) littermates using microdialysis. At 4 weeks of age, there were no differences in basal releases of glutamate and GABA during wakefulness and SWS between non-TG and S284L-TG. The switching from wakefulness to SWS affected neither glutamate nor GABA releases in both groups of littermates (Fig. 10*a*). At 8 weeks of age, the basal glutamate release of S284L-TG was greater than that of non-TG during both wakefulness and SWS, whereas there was no difference in basal GABA release during wakefulness and SWS between non-TG and S284L-TG (Fig. 10*b*). The switching from wakefulness to SWS reduced glutamate release without changing GABA release in non-TG, but, in S284L-TG, neither glutamate nor GABA releases were changed (Fig. 10*b*). During interictal discharge, glutamate release in the focus region was increased, but GABA release was stable (Fig. 10*b*).

The release of both glutamate and GABA increased in the focus region by spontaneous seizure (epileptic wandering) (Fig. 10*c*). We demonstrated epileptic wandering associated with a transient surge in frontal glutamate and GABA releases (Fig. 10*c*); the increase in GABA release was preceded by that in glutamate. At the end of epileptic wandering, glutamate level returned to the pre-event level, whereas that of GABA showed some delay (Fig. 10*c*).

Discussion

The phenotypic features of S284L-TG were similar to the clinical features of human ADNFLE, which are (1) seizures with a frontal semiology, (2) seizures during sleep, (3) absence of neurological deficits, (4) normal findings on neuroimaging, and (5) an autosomal dominant mode of inheritance (Tassinari and Michelucci, 1997; Provini et al., 1999; Combi et al., 2004). The S284L-TG thus exhibited three distinct spontaneous seizures during SWS similar to those of ADNFLE/NFLE (Provini et al., 1999; Combi et al., 2004). Electrocorticography clearly indicated that the dominant seizures in S284L-TG originated from the frontal sensorimotor cortex during SWS. As expected, S284L-TG showed autosomal dominant inheritance in accordance with Mendelian expectations. No abnormality of S284L-TG was found in several histological and behavioral screening tests.

Rats were chosen as a target animal in this study considering future usage because basic experiments in epileptology have been mainly conducted in rats. In this study, a transgenic genetic method rather than knock-in strategy was exploited, because knock-in engineering is not, if at all, yet applicable to rats. The genetic integrity of transgenic animals may be argued. The transgenic approach, however, is especially suitable when products of transgenes exert dominant-negative effect. Autosomal dominant inheritance in ADNFLE is the case because the mutant α4 subunit is incorporated in hetero-pentameric nAChR in which it ham-

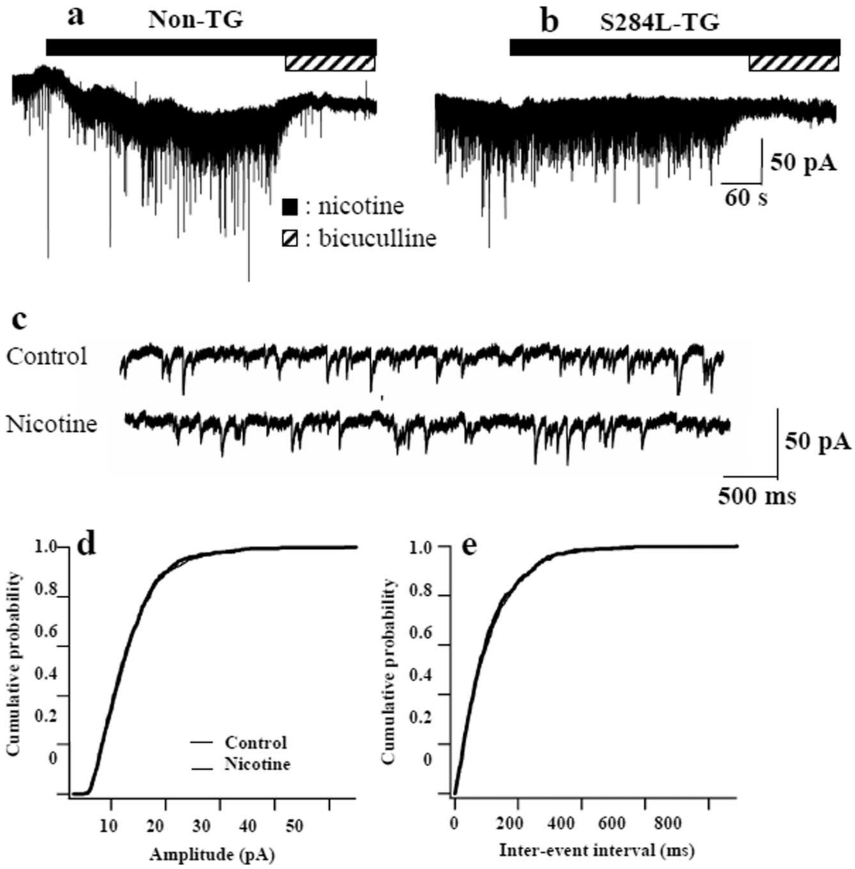

Figure 8. Nicotine (10 μM) increased the amplitude and frequency of sIPSC followed by marked inward shift of baseline of cortical layer V pyramidal neurons in non-TG (***a***) but only induced a small inward shift in S284L-TG (***b***). The nicotine-induced sIPSC and inward shift of baseline (tonic inhibition) were abolished by $GABA_A$ receptor antagonist (10 μM bicuculline). ***c***, Typical responses of sensorimotor cortical layer II/III pyramidal neurons of S284L-TG to 10 min application of 10 μM nicotine. During sIPSC monitoring, to inhibit the muscarinic, α7-nAChR, glutamatergic (NMDA and AMPA), and $GABA_B$ receptors, we used ACSF containing atropine (1 μM), MLA (0.1 μM), D-APV (50 μM), CNQX (10 μM), and CGP55845 (3 μM), respectively. After recording of control data (top black trace), the superfusion medium was changed to the same ACSF containing 10 μM nicotine (bottom gray trace). Cumulative probability distributions for IPSC frequency and peak amplitude of control (thin lines) and during application of nicotine (thick lines, ***d***, ***e***). Nicotine did not alter the peak amplitude or interevent interval of sIPSC of pyramidal neurons in layer II/III (Kolmogorov–Smirnoff test) similar to that in layer V (Fig. 7*a–f*).

pers the function of the receptor altogether. The mutant *Chrna4* was selectively expressed in the cortex and hippocampus of S284L-TG, but the amount of mRNA of the mutant *Chrna4* in S284L-TG was comparable with that of the wild-type *Chrna4* in the focus region. More importantly, no abnormalities of distorted expression of transgene were detected in either neurons or glia of S284L-TG. These findings indicate that the expression of S284L mutant $\alpha 4\beta 2$-nAChR in the sensorimotor cortex plays an important role in the pathogenesis of nocturnal frontal lobe epilepsy.

Human ADNFLE/NFLE usually appears before puberty, and ~88% of ADNFLE patients had the first seizure before the age of 20 (Tassinari and Michelucci, 1997; Provini et al., 1999; Combi et al., 2004). Similarly, interictal discharge and spontaneous seizure appeared at 6 weeks in S284L-TG (before breeding stage). Furthermore, similar to partial epilepsy in human (During and Spencer, 1993; During et al., 1995), epileptic wandering in S284L-TG was associated with a transient surge in glutamate and GABA releases.

$\alpha 4\beta 2$-nAChRs and α7-nAChRs facilitate GABAergic and glutamatergic transmissions in many brain regions, respectively (Gil et al., 1997; Léna and Changeux, 1997; MacDermott et al., 1999). Our slice patch-clamp experiments revealed that $\alpha 4\beta 2$-nAChR in S284L-TG had loss of function for activation of GABAergic transmission in both synaptic (sIPSC) and extrasynaptic (tonic inhibition) inhibitions without changing sEPSC, in pyramidal neurons of sensorimotor cortical layers II/III and V (focus region) without affecting excitatory glutamatergic sEPSC. Previous electrophysiological studies with reconstituted $\alpha 4\beta 2$-nAChR on *Xenopus* oocytes demonstrated that S284L enhanced steady-state desensitization to ACh response of the receptor (Matsushima et al., 2002; Rodrigues-Pinguet et al., 2003). Thus, attenuated GABAergic transmission via rapid desensitization (Matsushima et al., 2002; Rodrigues-Pinguet et al., 2003) and unchanged glutamatergic transmission in sensorimotor cortical pyramidal neurons are suggested in S284L-TG. These changes of GABAergic transmission in TG rat might be involved in the manifestation of seizure or the enhanced propagation of neuronal excitability in the sensorimotor cortex of S284L-TG. In contrast, nicotine application activated pre- and/or post-nAChRs, followed by Ca^{2+} influx. Consequently, nicotine application augmented GABAergic transmission in non-TG.

Controversial data exist about the sensitivity of ADNLF mutants for ACh, which point to increased ACh sensitivity without profound desensitization (Bertrand et al., 2002). The present mutant S284L displayed rapid desensitization (Matsushima et al., 2002; Rodrigues-Pinguet et al., 2003), and the mutant failed to facilitate the nicotine-induced GABAergic transmission. These data suggest that S284L mutant has reduced sensitivity to ACH. The reason for this fundamental difference is still unknown. Additional studies are required to determine the mechanism of dysfunction of GABAergic transmission via S284L mutant nAChR, because ADNLF mutant nAChR-mediated regulation of GABAergic transmission depends on several factors such as sensitivity to ACh of mutant nAChR, locations of nAChR (presynaptic or postsynaptic, excitatory or inhibitory neurons), and desensitization of AChR by the application system. Therefore, more sophisticated approaches such as double patch technique using a rapid application system, allowing simultaneous recording of pyramidal cells and interneurons, could perhaps narrow the differences.

In the present study, electrophysiological experiments were performed using 4-week-old rat. The electrophysiological data demonstrated not only alterations of nAChR-mediated responses but also dysfunction of GABAergic transmission. Furthermore, these phenotypic changes were established before seizure episodes. In particular, dysfunction of GABAergic transmission might play an important role in epileptogenesis before seizure age. Indeed, there is evidence to suggest that the epileptic model animal showed GABAergic dysfunction.

Despite impaired nicotine-induced GABA release in S284L-

TG, we found a transient rise in GABA release associated with epileptic wandering. In particular, increased GABA release associated with epileptic wandering was delayed compared with that of glutamate. This discrepancy suggests that the neuronal hyperactivation associated with epileptic wandering is affected by not only the dysfunctional ACh-ergic transmission but also that of glutamate and GABA.

Two abnormalities of frontal neurotransmitter releases in relation to the circadian rhythm emerged after the appearance of interictal discharge and spontaneous seizures during SWS (8 weeks of age), which were not observed at the preclinical stage (4 weeks of age). The first was that the basal glutamate release in the focus region of S284L-TG was greater than that of non-TG during both wakefulness and SWS. The second was lack of the reduction of glutamate release during sleep in sensorimotor cortex, which is normally observed at 8 weeks of age (no such reduction in glutamate release was observed at 4 weeks of age). Therefore, the pronounced excitatory transmission associated with sleep in the focus region might play a role in the origination of interictal discharges or spontaneous epileptic seizures.

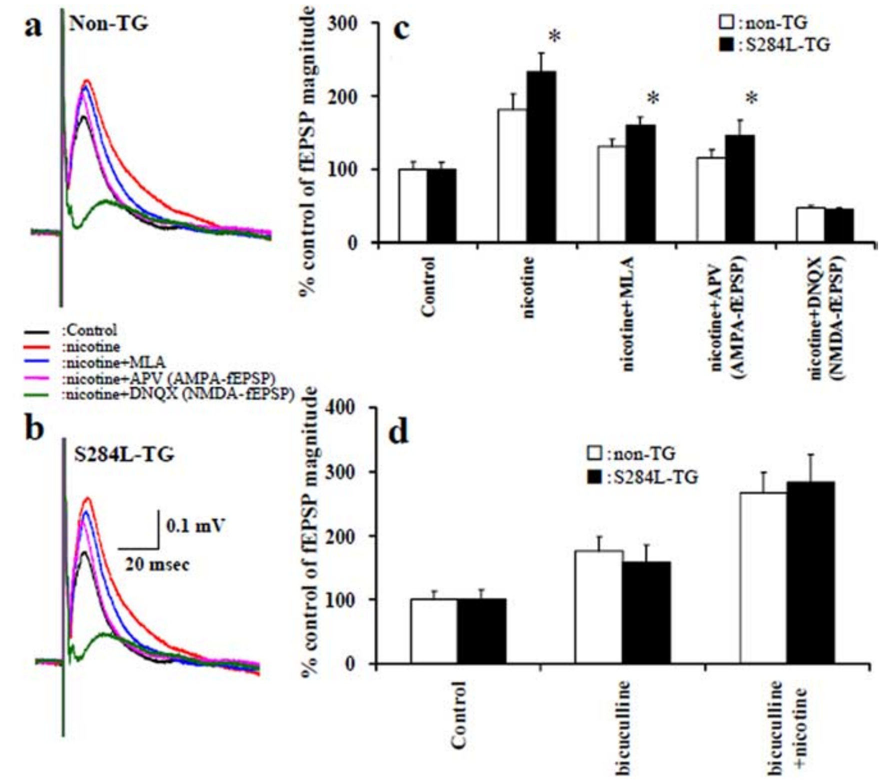

Figure 9. ***a***, ***b***, fEPSPs in the sensorimotor cortex were monitored using MED64. The top (non-TG; ***a***) and bottom (S284L-TG; ***b***) traces of the sensorimotor cortex indicate the effects of 10 μM nicotine, the inhibitors of α7-nAChR MLA (0.1 μM), NMDA receptor D-APV (50 μM), and AMPA receptor 6,7-dinitroquinoxaline-2.3-dione (DNQX, 20 μM) on fEPSPs. ***c***, Effects of superfusion with 1 μM (1) and 10 μM (10) nicotine on amplitude of fEPSPs in the sensorimotor cortex. Data are mean $\pm$ SD of six rats. *$p < 0.05$, **$p < 0.01$ (Student's *t* test). ***d***, Interaction between bicuculline (10 μM) and nicotine (10 μM) on magnitude of fEPSPs in the sensorimotor cortex. Data are mean $\pm$ SD of six rats. *$p < 0.05$, **$p < 0.01$ (Student's *t* test).

Two knock-in mouse models of ADNFLE have been described recently (Klaassen et al., 2006). The two models bear heterozygous mutations of *Chrna4*, either S280F or insL, which are homologous to mutations found in ADNFLE but different from those of S284L. Both knock-in mouse models exhibited seizure phenotypes, including spontaneous seizures during sleep, similar to those observed in human ADNFLE. However, the reported seizure phenotype apparently resembled epileptic wondering, although the other phenotypes characteristic of NFLE, i.e., paroxysmal arousal and nocturnal dystonia, were not described (Klaassen et al., 2006).

Surprisingly, contrary to S284L-TG, the main functional abnormality in the knock-in mice was enhanced cortical GABAergic inhibition in layers II/III of the frontal lobe (Klaassen et al., 2006). The findings are in contrast to our results in S284L-TG rats in which attenuation of both intrasynaptic and extrasynaptic GABAergic transmission in layers II/III and V was observed.

An association between epileptic seizure and enhanced GABAergic inhibition has been already observed in temporal lobe epilepsy models (Chen et al., 1999). Although the developmental or subcortical abnormalities of these two knock-in mice should be ruled out, the functional abnormality, hypersynchronized GABAergic inhibition, plays important roles in ADNFLE seizure with S280F and insL (Klaassen et al., 2006; Mann and Mody, 2008). In this regard, the GABAergic functional abnormalities of mutated $\alpha4\beta2$-nAChR identified in individuals with ADNFLE/NFLE vary despite the apparent homogenous clinical presentation with a few variations. Additional studies using mice bearing S280F or insL and S284L-TG provide a deeper understanding regarding the pathogenic mechanisms underlying ADNFLE/NFLE resulting from impaired and enhanced GABAergic functional abnormalities.

The unique sensitivity of ADNFLE to antiepileptic drugs caused by S284L is one of a few variations known in the ADNFLE/NFLE semiology. Thus, carbamazepine remains the first-choice antiepileptic drug for treatment of ADNFLE/NFLE; however, ADNFLE/NFLE patients with S284L respond only partially to carbamazepine but are more susceptible to zonisamide or benzodiazepine (Provini et al., 1999; Ito et al., 2000; Combi et al., 2004). Both carbamazepine and zonisaminde exert their antiepileptic activity by inhibiting Na^+ channel. Bertrand et al. (2002) demonstrated that $\alpha4\beta2$-nAChR with S280F, insL, and V287M mutation displayed increased sensitivity to carbamazepine, whereas $\alpha4\beta2$-nAChR with S284L mutant did not exhibit this feature (Bertrand et al., 2002). The present study also demonstrated that diazepam and zonisamide but not carbamazepine reduced the interictal discharges in S284L-TG similar to ADNFLE patients with S284L mutation. Therefore, the impaired sensitivity to carbamazepine of S284L-TG is possibly modulated by the receptor binding profile of nAChR with S284L mutation. Additionally, diazepam and zonisamide but not carbamazepine enhances $GABA_A$ receptor activities (Rusakov and Fine, 2003; Yoshida et al., 2005). Both electrophysiological and pharmacological results suggest that the reduced GABAergic transmission in S284L-TG was compensated by enhancement of GABAergic transmission by zonisamide but not carbamazepine. Additional studies are needed to determine the pathomechanisms of the different sensitivities between ADNFLE/NFLE with S284L and other mutations.

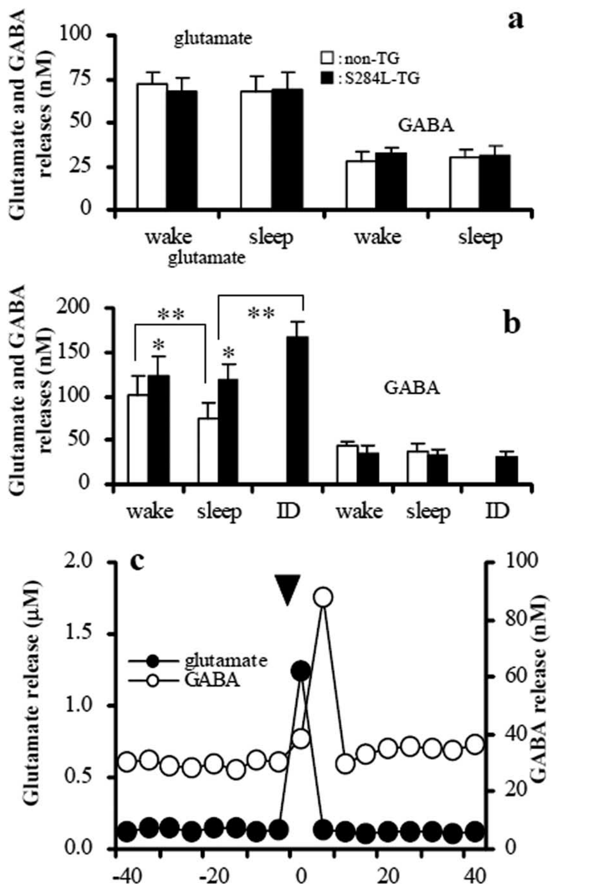

Figure 10. ***a***, Release of glutamate and GABA in the frontal cortex during wakefulness (wake) and SWS (sleep) at 4 weeks age. Data are mean ± SD of eight rats in each group (one-way ANOVA with Tukey's multiple comparison). ***b***, Release of glutamate and GABA in the frontal cortex during wakefulness (wake), SWS (sleep), and interictal discharge (ID) at 8 weeks of age. Data are mean ± SD of nine rats in each group. $^{*}p < 0.05$, $^{**}p < 0.01$ (one-way ANOVA with Tukey's multiple comparison). ***c***, Release of glutamate and GABA in the frontal cortex of S284L-TG during epileptic wandering. Abscissa, Time before (negative values) and after (positive values) onset of epileptic wandering (blue arrow).

In conclusion, the underlying abnormalities in neurotransmission of S284L TG were (1) attenuation of synaptic and extrasynaptic GABAergic transmission and (2) abnormal glutamate release during sleep.

References

Aramakis VB, Metherate R (1998) Nicotine selectively enhances NMDA receptor-mediated synaptic transmission during postnatal development in sensory neocortex. J Neurosci 18:8485–8495.

Aridon P, Marini C, Di Resta C, Brilli E, De Fusco M, Politi F, Parrini E, Manfredi I, Pisano T, Pruna D, Curia G, Cianchetti C, Pasqualetti M, Becchetti A, Guerrini R, Casari G (2006) Increased sensitivity of the neuronal nicotinic receptor alpha 2 subunit causes familial epilepsy with nocturnal wandering and ictal fear. Am J Hum Genet 79:342–350.

Bayazitov I, Kleschevnikov A (2000) Afferent high strength tetanizations favour potentiation of the NMDA vs. AMPA receptor-mediated component of field EPSP in CA1 hippocampal slices of rats. Brain Res 866:188–196.

Bertrand D, Picard F, Le Hellard S, Weiland S, Farve I, Phillips H, Bertrand S, Berkovic SF, Malafosse A, Mulley J (2002) How mutations in the nAChRs can cause ADNFLE Epilepsy. Epilepsia [Suppl] 43:112–122.

Bertrand D, Elmslie F, Hughes E, Trounce J, Sander T, Bertrand S, Steinlein OK (2005) The CHRNB2 mutation I312M is associated with epilepsy and distinct memory deficits. Neurobiol Dis 20:799–804.

Chen K, Baram TZ, Soltesz I (1999) Febrile seizures in the developing brain result in persistent modification of neuronal excitability in limbic circuits. Nat Med 5:888–894.

Combi R, Dalprà L, Tenchini ML, Ferini-Strambi L (2004) Autosomal dominant nocturnal frontal lobe epilepsy—a critical overview. J Neurol 251:923–934.

Connors BW (1997) Neocortical anatomy and physiology. In: A comprehensive textbook of epilepsy (Engel J Jr, Pedley TA, eds), pp 307–321. Philadelphia: Lippincott-Raven.

De Fusco M, Becchetti A, Patrignani A, Annesi G, Gambardella A, Quattrone A, Ballabio A, Wanke E, Casari G (2000) The nicotinic receptor b2 subunit is mutant in nocturnal frontal lobe epilepsy. Nat Genet 26:275–276.

During MJ, Spencer DD (1993) Extracellular hippocampal glutamate and spontaneous seizure in the conscious human brain. Lancet 341:1607–1610.

During MJ, Ryder KM, Spencer DD (1995) Hippocampal GABA transporter function in temporal-lobe epilepsy. Nature 376:174–177.

Farrant M, Nusser Z (2005) Variations on an inhibitory theme: phasic and tonic activation of $GABA_A$ receptors. Nat Rev Neurosci 6:215–229.

Gil Z, Connors BW, Amitai Y (1997) Differential regulation of neocortical synapses by neuromodulators and activity. Neuron 19:679–686.

Glykys J, Mody I (2007) The main source of ambient GABA responsible for tonic inhibition in the mouse hippocampus. J Physiol 582:1163–1178.

Harasawa I, Honda K, Tanoue A, Shinoura H, Ishida Y, Okamura H, Murao N, Tsujimoto G, Higa K, Kamiya HO, Takano Y (2003) Responses to noxious stimuli in mice lacking alpha(1d)-adrenergic receptors. Neuroreport 14:1857–1860.

Hase K, Ohshima S, Kawano K, Hashimoto N, Matsumoto K, Saito H, Ohno H (2005) Distinct gene expression profiles characterize cellular phenotypes of follicle-associated epithelium and m cells. DNA Res 12:127–137.

Hirano K, Kimura R, Sugimoto Y, Yamada J, Uchida S, Kato Y, Hashimoto H, Yamada S (2005) Relationship between brain serotonin transporter binding, plasma concentration and behavioural effect of selective serotonin reuptake inhibitors. Br J Pharmacol 144:695–702.

Hirose S, Iwata H, Akiyoshi H, Kobayashi K, Ito M, Wada K, Kaneko S, Mitsudome A (1999) A novel mutation of *CHRNA4* responsible for autosomal dominant nocturnal frontal lobe epilepsy. Neurology 53:1749–1753.

Ito M, Kobayashi K, Fujii T, Okuno T, Hirose S, Iwata H, Mitsudome A, Kaneko S (2000) Electroclinical picture of autosomal dominant nocturnal frontal lobe epilepsy in a Japanese family. Epilepsia 41:52–58.

Klaassen A, Glykys J, Maguire J, Labarca C, Mody I, Boulter J (2006) Seizures and enhanced cortical GABAergic inhibition in two mouse models of human autosomal dominant nocturnal frontal lobe epilepsy. Proc Natl Acad Sci U S A 103:19152–19157.

Kuteeva E, Calza L, Holmberg K, Theodorsson E, Ogren SO, Hökfelt T (2004) Distribution of galanin and galanin transcript in the brain of a galanin-overexpressing transgenic mouse. J Chem Neuroanat 28:185–216.

Le Novère N, Zoli M, Changeux JP (1996) Neuronal nicotinic receptor alpha 6 subunit mRNA is selectively concentrated in catecholaminergic nuclei of the rat brain. Eur J Neurosci 8:2428–2439.

Léna C, Changeux JP (1997) Role of Ca^{2+} ions in nicotinic facilitation of GABA release in mouse thalamus. J Neurosci 17:576–585.

Leniger T, Kananura C, Hufnagel A, Bertrand S, Bertrand D, Steinlein OK (2003) A new Chrna4 mutation with low penetrance in nocturnal frontal lobe epilepsy. Epilepsia 44:981–985.

MacDermott AB, Role LW, Siegelbaum SA (1999) Presynaptic ionotropic receptors and the control of transmitter release. Annu Rev Neurosci 22:443–485.

Matsushima N, Hirose S, Iwata H, Fukuma G, Yonetani M, Nagayama C, Hamanaka W, Matsunaka Y, Ito M, Kaneko S, Mitsudome A, Sugiyama H (2002) Mutation (Ser284Leu) of neuronal nicotinic acetylcholine receptor alpha 4 subunit associated with frontal lobe epilepsy causes faster desensitization of the rat receptor expressed in oocytes. Epilepsy Res 48:181–186.

Mishima K, Tanoue A, Tsuda M, Hasebe N, Fukue Y, Egashira N, Takano Y, Kamiya HO, Tsujimoto G, Iwasaki K, Fujiwara M (2004) Characteristics of behavioral abnormalities in alpha1d-adrenoceptors deficient mice. Behav Brain Res 152:365–373.

Mori F, Okada M, Tomiyama M, Kaneko S, Wakabayashi K (2005) Effects of ryanodine receptor activation on neurotransmitter release and neuronal cell death following kainic acid-induced status epilepticus. Epilepsy Res 65:59–70.

Nakatsu F, Okada M, Mori F, Kumazawa N, Iwasa H, Zhu G, Kasagi Y, Kamiya H, Harada A, Nishimura K, Takeuchi A, Miyazaki T, Watanabe M, Yuasa S, Manabe T, Wakabayashi K, Kaneko S, Saito T, Ohno H (2004) Defective function of GABA-containing synaptic vesicles in mice lacking the AP-3B clathrin adaptor. J Cell Biol 167:293–302.

Nakayama H, Shioda S, Okuda H, Nakashima T, Nakai Y (1995) Immunocytochemical localization of nicotinic acetylcholine receptor in rat cerebral cortex. Brain Res Mol Brain Res 32:321–328.

Okada M, Nutt DJ, Murakami T, Zhu G, Kamata A, Kawata Y, Kaneko S (2001) Adenosine receptor subtypes modulate two major functional pathways for hippocampal serotonin release. J Neurosci 21:628–640.

Okada M, Zhu G, Hirose S, Ito KI, Murakami T, Wakui M, Kaneko S (2003) Age-dependent modulation of hippocampal excitability by KCNQ-channels. Epilepsy Res 53:81–94.

Phillips HA, Marini C, Scheffer IE, Sutherland GR, Mulley JC, Berkovic SF (2000) A de novo mutation in sporadic nocturnal frontal lobe epilepsy. Ann Neurol 48:264–267.

Phillips HA, Favre I, Kirkpatrick M, Zuberi SM, Goudie D, Heron SE, Scheffer IE, Sutherland GR, Berkovic SF, Bertrand D, Mulley JC (2001) CHRNB2 is the second acetylcholine receptor subunit associated with autosomal dominant nocturnal frontal lobe epilepsy. Am J Hum Genet 68:225–231.

Provini F, Plazzi G, Tinuper P, Vandi S, Lugaresi E, Montagna P (1999) Nocturnal frontal lobe epilepsy. A clinical and polygraphic overview of 100 consecutive cases. Brain 122:1017–1031.

Rodrigues-Pinguet N, Jia L, Li M, Figl A, Klaassen A, Truong A, Lester HA, Cohen BN (2003) Five ADNFLE mutations reduce the Ca^{2+} dependence of the mammalian a4b2 acetylcholine response. J Physiol 550:11–26.

Rossi DJ, Hamann M, Attwell D (2003) Multiple modes of GABAergic inhibition of rat cerebellar granule cells. J Physiol 548:97–110.

Rusakov DA, Fine A (2003) Extracellular Ca^{2+} depletion contributes to fast activity-dependent modulation of synaptic transmission in the brain. Neuron 37:287–297.

Schröder H, Zilles K, Maelicke A, Hajós F (1989) Immunohisto- and cytochemical localization of cortical nicotinic cholinoceptors in rat and man. Brain Res 502:287–295.

Steinlein OK, Mulley JC, Propping P, Wallace RH, Phillips HA, Sutherland GR, Scheffer IE, Berkovic SF (1995) A missense mutation in the neuronal nicotinic acetylcholine receptor alpha 4 subunit is associated with autosomal dominant nocturnal frontal lobe epilepsy. Nat Genet 11:201–203.

Steinlein OK, Magnusson A, Stoodt J, Bertrand S, Weiland S, Berkovic SF, Nakken KO, Propping P, Bertrand D (1997) An insertion mutation of the CHRNA4 gene in a family with autosomal dominant nocturnal frontal lobe epilepsy. Hum Mol Genet 6:943–947.

Steinlein OK, Stoodt J, Mulley J, Berkovic S, Scheffer IE, Brodtkorb E (2000) Independent occurrence of the CHRNA4 Ser248Phe mutation in a Norwegian family with nocturnal frontal lobe epilepsy. Epilepsia 41:529–535.

Tassinari CA, Michelucci R (1997) Familiar frontal and temporal lobe epilepsy. Philadelphia: Lippincott-Raven.

Tecott LH, Sun LM, Akana SF, Strack AM, Lowenstein DH, Dallman MF, Julius D (1995) Eating disorder and epilepsy in mice lacking 5-HT_{2C} serotonin receptors. Nature 374:542–546.

Wonnacott S (1997) Presynaptic nicotinic ACh receptors. Trends Neurosci 20:92–98.

Yamamoto S, Yamada J, Ueno S, Kubota H, Furukawa T, Yamamoto S, Fukuda A (2007) Insertion of α7 nicotinic receptors at neocortical layer V GABAergic synapses is induced by a benzodiazepine, midazolam. Cereb Cortex 17:653–660.

Yoshida S, Okada M, Zhu G, Kaneko S (2005) Effects of zonisamide on neurotransmitter exocytosis associated with ryanodine receptors. Epilepsy Res 67:153–162.

Zucker B, Luthi-Carter R, Kama JA, Dunah AW, Stern EA, Fox JH, Standaert DG, Young AB, Augood SJ (2005) Transcriptional dysregulation in striatal projection- and interneurons in a mouse model of Huntington's disease: neuronal selectivity and potential neuroprotective role of HAP1. Hum Mol Genet 14:179–189.